

DESIGN CONSIDERATIONS FOR AN MEBT CHOPPER ABSORBER OF 2.1MEV H- AT THE PROJECT X INJECTOR EXPERIMENT AT FERMILAB*

C. Baffes,[#] M. Awida, A. Chen, Y. Eidelman, V. Lebedev, L. Prost, A. Shemyakin, N. Solyak, V. Yakovlev, FNAL, Batavia, IL 60510, USA

Abstract

The Project X Injector Experiment (PXIE) [1] will be used to validate the Project X front end design concept. One of the most challenging components of PXIE is the wide-band chopping system of the Medium Energy Beam Transport (MEBT) section, which will form an arbitrary bunch pattern from the initially CW 162.5 MHz 5mA beam. The present scenario assumes diverting 80% of the beam to an absorber to provide a beam with the average current of 1mA to the SRF linac. This absorber must withstand a high level of energy deposition and high ion fluence, while being positioned in proximity of the superconductive cavities. This paper discusses design considerations for the absorber. Thermal and mechanical analyses of a conceptual design are presented, and plans for the fabrication and testing of a prototype are described.

CONFIGURATION AND CHALLENGES

The PXIE MEBT accepts a 2.1MeV, 162.5MHz CW beam with the current up to 10 mA (nominal 5mA) and forms a desired arbitrary bunch structure with the average (over ~1 μs) beam current of 1 mA by directing undesired bunches to the MEBT beam absorber (Fig.1). Some of the key absorber requirements are summarized in Table 1.

Table 1: MEBT Absorber Requirements

| Species/Energy | H- @ 2.1 MeV |
|--------------------------|------------------------|
| Nominal absorbed current | 4mA |
| Maximum absorbed current | 10mA (design value) |
| Maximum absorbed power | 21 kW |
| RMS beam transverse size | 2 mm |
| Maximum length | 650mm flange-to-flange |

Challenges presented by the absorber design include maintaining vacuum quality, managing surface effects (sputtering and blistering), containing secondary particles, accommodating radiation effects, spreading energy deposition, and the survival of temperatures and temperature-induced mechanical stresses. At a beam energy of 2.1MeV the mean stopping length is about 20μm. Therefore heating of the absorber is essentially a surface phenomenon. To limit power density, the beam is directed to the absorber at the grazing angle of 29mrad. This spreads the beam energy out over a length of ~400mm (±3σ). Even so, the maximum power flux at the

absorber surface is 22W/mm² for the 10mA beam. If improperly addressed, this could result in unacceptably high local temperatures and mechanical stresses, as well as severe surface degradation.

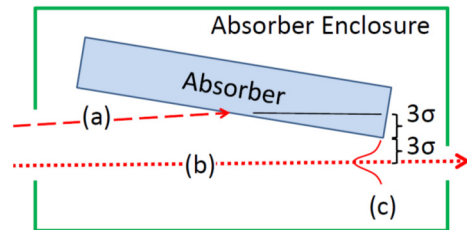


Figure 1: Schematic representation of the absorber showing (a) chopped beam, (b) passed beam, (c) beam profile and 6σ transverse shift between the centers of the chopped and passed beams.

BEAM-INDUCED EROSION AND MATERIAL CHOICE

Surface blistering of metals exposed to low energy (E<200keV) ion beams is well documented in the literature (e.g. [2]). Ions are implanted just below the surface of the material by the beam and combine to form Hydrogen gas. Pockets of the gas coalesce, eventually erupting through the surface. These eruptions release concentrated bursts of gas and create physical debris, eroding the metal surface in the process. Both gas bursts and debris generation would be particularly undesirable in this application.

The severity of blistering is influenced by a number of factors including beam parameters (current density, particle fluence, particle energy), material parameters (hydrogen solubility, diffusion rates), and physical parameters (temperature, surface roughness). The geometry and beam parameters of the MEBT absorber will result in a peak particle flux of approximately 7E19 particles/m²/s. This is a severe condition for many materials. For example, the blistering threshold (the fluence at which blisters first appear) for copper has been reported to be of order 4E21 particles/m² [2]. The MEBT absorber would reach this threshold is less than 1 minute of operation.

This motivated the search for a suitable material for use in the absorber. The properties considered in this trade were blistering resistance, thermal conductivity, temperature capability, high-temperature strength characteristics, machinability, cost, and availability in the desired sizes. Two-material solutions were considered, most plausibly a thin layer of blistering-resistant (but low-thermal-conductivity) tantalum over a substrate of

* Operated by Fermi Research Alliance, LLC, under Contract DE-AC02-07CH11359 with the United States Department of Energy.

[#]cbaffes@fnal.gov

high-thermal conductivity copper. However, these solutions were not pursued due to concerns about the fabrication and robustness of the material interface. For a single-material monolithic absorber, a good compromise between blistering resistance, thermal/mechanical properties, and cost is achieved with the Molybdenum alloy TZM. TZM has been shown to be blistering resistant up to fluences of $1E24$ particles/m² [3],[4]. TZM also offers good thermal conductivity (120 W/m²K) and high temperature capability (recrystallization temp approx. 1400°C).

Sputtering of the absorber surface was calculated using the SRIM code [5]. Peak sputtering erosion for TZM (at the center of the beam profile and assuming 10mA absorbed current) is estimated to be of order 1 μ m per day. This can be compared to the characteristic ion implantation/blistering depth of 0.6 μ m (measured normal to the absorber surface). If blistering can be resisted for an adequate length of time, sputtering may continually remove the affected material and expose fresh material beneath.

ABSORBER GEOMETRY

In order to minimize fabrication risk, the absorber will consist of four identical modules, each 125mm long. Analysis (to be discussed in the following section) indicated that beam heating caused high compressive stresses on the surface of the absorber. In order to relieve these stresses, thin slits are cut in the transverse direction, allowing for local expansion of the hot outer fiber. However, the fabrication of these slits will create surfaces nearly perpendicular to the beam direction. If the beam hits such a surface at near-normal angle of incidence, the local energy deposition would be high enough to cause melting. To avoid this, step height increments are machined into the surface of the absorber. These steps "shadow" the vertical surfaces to protect them from near-normal beam. An analogous height increment is implemented between absorber modules.

In order to cool the absorber surface, water flows through the TZM material transverse to the beam direction. The cooling channels are densely packed to limit heat flux to the water (to about 1W/mm²) and avoid boiling thresholds. The high-aspect-ratio EDM-machined channels will support laminar flow at 1-2m/s. The 16mm facesheet thickness (between the surface and the cooling channels) allows heat to spread out in the radial direction before flowing into the coolant.

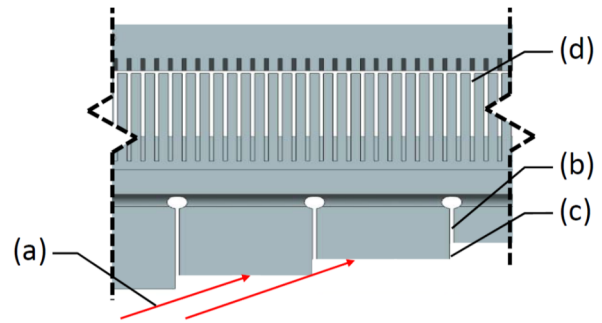


Figure 2: Side view of absorber showing (a) beam incident on surface, (b) axial stress relief slits, (c) shadowing step increment (magnitude exaggerated), (d) 300 μ m wide by 1mm pitch water cooling channels. Horizontal scale exaggerated.

THERMAL AND STRESS ANALYSIS

Preliminary thermal analysis of the absorber has been performed in ANSYS [6], assuming the maximum beam power of 21 kW. Heating was modeled as a surface heat flux from a Gaussian beam projected onto the surface at the grazing angle of incidence. Heat flux was applied to surface nodes using a do-loop architecture.

Convection in the water channels was modeled using a constant average convection coefficient of 6500 W/m²°K, based on empirical Nusselt number correlations for high-aspect ratio channels presented in [7]. A stand-alone fluids model was used to assess and optimize flow characteristics, channel-to-channel flow uniformity, and along-streamline heating of the water.

Temperature and stress are shown in Figure 3. Maximum temperatures on the absorber surface are about 1050°C, with a strong radial temperature gradient. Due to the small angle of incidence, axial temperature variations are gradual over the length scale of the axial stress relief slit pitch (1cm).

High stresses are observed in two areas. At the absorber surface, a compressive stress develops as the heated material on the surface expands and is resisted by the cooler material around it. The magnitude of this effect is limited by the presence of the axial stress relief slits. A second area of high stress is present at the root of the axial stress relief slits, where global thermal expansion of the absorbing surface is resisted by bending and tension in the cool material below. Stress at the root of the slit is minimized by a generous fillet.

Though stresses and temperatures within the absorber will be high, the TZM material offers good mechanical properties under these conditions. As shown in the Figure 4, peak stress and temperature conditions are below the temperature-dependent yield curve for TZM.

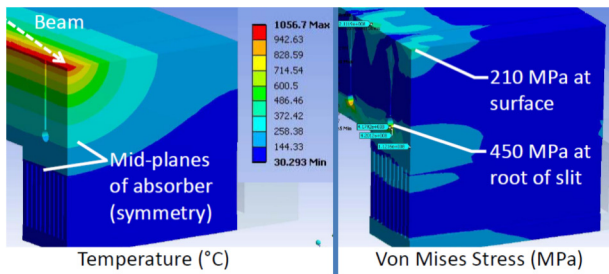


Figure 3: Simulated temperature and stress contours.

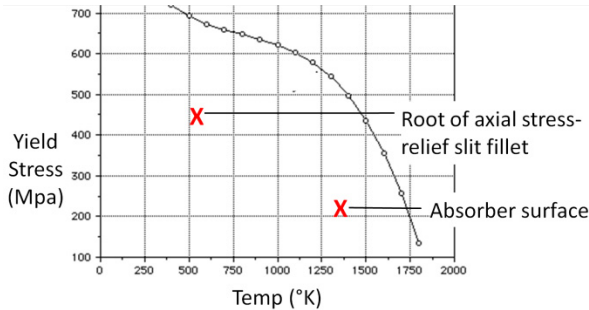


Figure 4: Stress/Temperature Conditions. Xs represent peak temperature (surface) and peak stress (slit) locations as compared to the TZM yield curve from [8].

ADDITIONAL CONSIDERATIONS

Vacuum and Gas Loading

As 4mA H⁺ beam arrives at the absorber, a significant amount of H₂ gas, 4×10⁻⁴ torr-l/s, will be produced. The gas load and sputtering pose challenges, considering that low pressure and low particulate conditions are desired just downstream at the cryomodule. In order to mitigate this risk, turbo pumps with total effective hydrogen pumping speed not less than 2500 l/s will be arranged so that 1) gas is pumped locally to minimize gas flux along the beamline; 2) pumps do not have line-of-sight to the sputtered surface, but still have adequate conductance; 3) a differential pumping scheme will be configured between absorber and the cryomodule so that a much lower residual gas pressure (down to 10⁻⁹ torr) can be achieved in the entry of the cryomodule; 4) a flow-regulated pumping/venting system will be implemented to reduce chance of particle or sputtered material migration.

Secondary Particles and Radiation

Due to the small incident angle a large fraction of the incoming beam protons will be scattered out of the absorber. This is beneficial for the thermal design of the absorber itself, because a fraction of the incident energy will be “reflected.” However, this will result in energy deposition at the walls of the absorber’s vacuum enclosure and downstream beam pipe that will require additional consideration.

Due to small beam energy (2.1MeV) neutron production and material activation are small. Neutron production will be of order 10⁻⁵ p/p; the primary reactions will be ¹⁰⁰Mo(p,n)¹⁰⁰Tc and ⁹⁷Mo(p,n)⁹⁷Tc.

ABSORBER CONFIGURATION IN PXIE

The MEBT absorber will consist of four identical modules, mounted to a common support structure. This structure will accommodate a static adjustment in position and angle relative to a mounting flange. The mounting flange will be installed from above into a vacuum enclosure, where vacuum pumps be mounted to as well. Optical diagnostics will monitor thermal and optical transition radiation from the beam absorber surface.

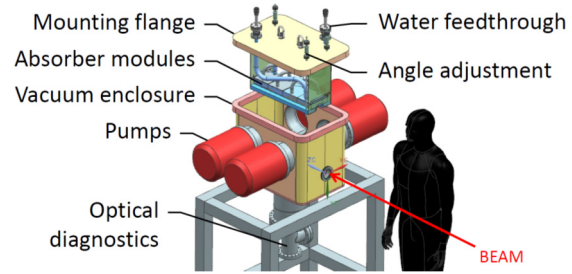


Figure 5: Exploded view of PXIE absorber.

TESTING PLANS

In advance of PXIE, a test absorber (single module) will be constructed. This module will reflect the geometry, materials, and manufacturing processes of the planned PXIE absorber. An existing electron beam gun will be used to replicate peak local power density at the absorber surface. This will provide an opportunity to validate the thermal performance and water flow characteristics of the absorber, and to correlate and improve the thermal analysis.

ACKNOWLEDGEMENTS

The authors wish to acknowledge the contributions of V. Dudnikov and T. Schenkel, who pointed out the importance of blistering and backscattering effects.

REFERENCES

- [1] V. Lebedev et al., Proc. of IPAC’12, New Orleans, USA, May 20-25, 2012, THPPP058; see also <http://www-bdnew.fnal.gov/PXIE/index.htm>
- [2] V.T. Astrelin et al., Journal of Nuclear Materials 396 p43, 2010 (see here for subject review refs.).
- [3] S.K. Das et al., Journal of Vacuum Science and Technology 15(2) p170, 1978.
- [4] Y. Nakamura, T. Shibata and M. Tanaka, Journal of Nuclear Materials 68 p253, 1977.
- [5] www.srim.org
- [6] www.ansys.com
- [7] W.M. Kays and M.E. Crawford, “Convection Heat and Mass Transfer,” McGraw-Hill, NYC, 1980.
- [8] T. E. Tietz and J. W. Wilson, "Behaviour and properties of refractory metals", Arnold Publishing Co, London (1965).